JOURNAL OF MATERIALS SCIENCE **38** (2003) 3747–3754

Metastable diamond synthesis from vitreous carbon and other disordered or nano-dispersed carbon materials

I. GUTZOW*
Institute of Physical Chemistry, Bulgarian Academy of Sciences, Sofia 1113, Bulgaria
E-mail: gutzow@ipc.bas.bg

S. TODOROVA
Geophysical institute, Bulgarian Academy of Sciences, Sofia 1113, Bulgaria

V. GUENCHEVA, E. GRANTSCHAROVA
Institute of Physical Chemistry, Bulgarian Academy of Sciences, Sofia 1113, Bulgaria

E. STOYANOV
Chemical Faculty, "St. Kliment Ohridski" University of Sofia, Sofia 1126, Bulgaria

L. KOSTADINOV
Institute of Physical Chemistry, Bulgarian Academy of Sciences, Sofia 1113, Bulgaria

G. BOGACHEV
Physical Faculty, "St. Kliment Ohridski" University of Sofia, Sofia1126, Bulgaria

B. RANGELOV, M. MARINOV
Institute of Physical Chemistry, Bulgarian Academy of Sciences, Sofia 1113, Bulgaria

K. HEIDE
Geological Institute, Friedrich Schiller Universität, 07743 Jena, Germany

A new method for growth of diamond seed crystals at metastable conditions is described. The process is realized isothermally (at temperatures in the range of 1000 K to 1400 K) in the closed volume of a quartz ampoule, via appropriate chemical transport reactions or in a CVD-apparatus. Vitreous carbon materials and other non-equilibrium forms of carbon, representing state of frozen-in disorder, increased thermodynamic potential and chemical affinity, are used as a constant driving force of isothermal crystallization.

The experiments are based on the detailed analysis of the thermodynamic properties of carbon modifications and on the influence of dispersity and the degree of disorder on their thermodynamic potential. Additional kinetic factors, influencing the diamond growth, like introduction of active substrates and mechanism of incorporation of carbon atoms in growing diamond face are also analyzed discussed in their possible technical application.

1. Introduction

In present-day artificial diamond synthesis two main possibilities are employed. First is diamond formation and growth at high pressures and temperatures, in the diamond stable region of the carbon phase diagram [1, 2]. Second comes metastable diamond growth at relatively low temperatures and normal pressure in the graphite stable field of the phase diagram [3–6]. The last possibility can be interpreted as being based on the predictions of Ostwald's Rule of Stages, especially in its kinetic interpretation in the framework of classical formulation of the nucleation theory [7–9]. The technical applications of the metastable diamond syntheses are realized in different variants of CVD processes [3, 6], taking place in temperature gradients, usually in the $C/H_2/H^*$ system [10–12].

Glasses and many other defect solids are from thermodynamic point of view non-equilibrium, frozen-in systems. In such systems not only a structure with increased disorder, but also a state with increased thermodynamic potential is frozen-in. This determines higher vapour pressure, solubility and chemical affinity of vitreous and vitreous-like solids [7, 13, 14]. Thus in such materials also the possibility is accumulated to be a sources of increased supersaturation in the processes of phase segregation and crystallization.

*Author to whom all correspondence should be addressed.

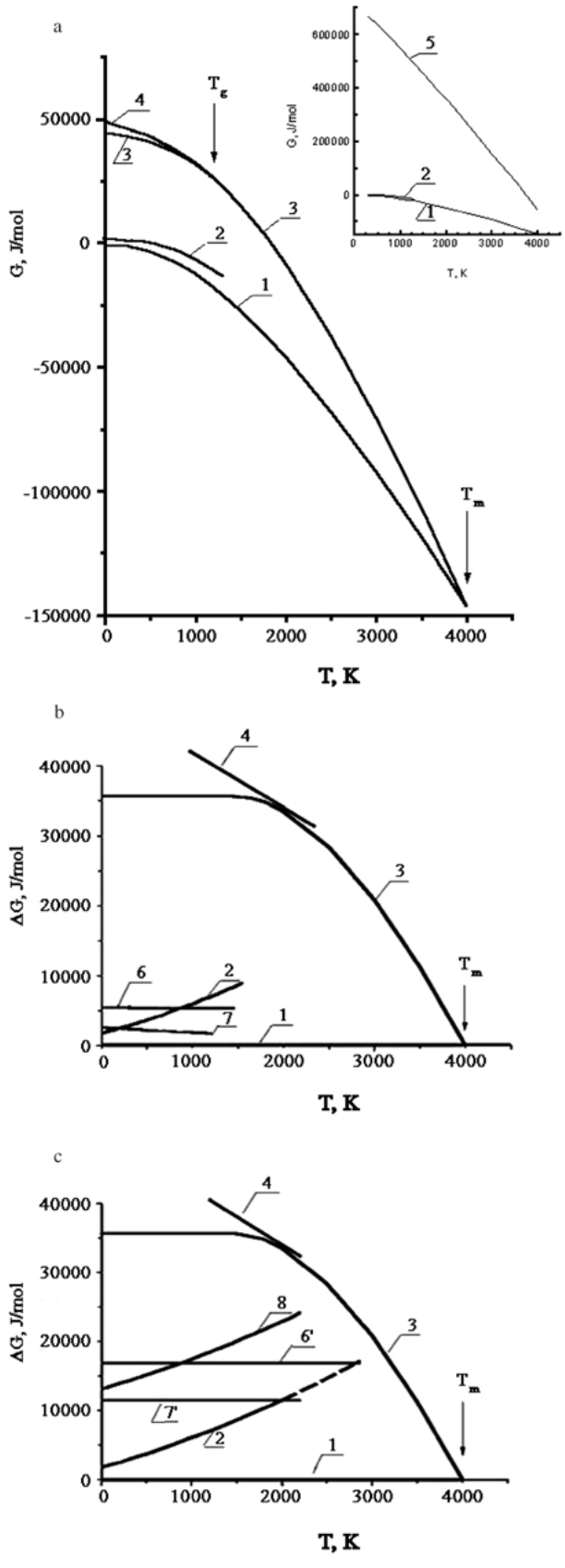

Figure 1 The thermodynamic properties of the different forms of carbon in terms of Gibbs' thermodynamic potential. (a) The temperature course of the thermodynamic potential $G_{gr}(T)$ of graphite (1), $G_d(T)$ of diamond (2), of the undercooled carbon melt (3) and of the hypothetical glass (4), formed from the undercooled melt at a glass transition temperature $T_g = (1/3)T_m$, where T_m is the melting temperature of graphite. In the insert is given the temperature dependence (5) of the thermodynamic potential $G_v(T)$ of carbon vapours. Note that the values of the differences $\Delta G_{v/gr}(T) = G_v(T) - G_{gr}(T)$ and of $\Delta G_{v/d}(T) = G_v(T) - G_d(T)$ are nearly equal. (b) The thermodynamic potential of the same forms of carbon as in a) in terms of the differences $\Delta G(T)$ (vs. $G_{gr}(T)$, given now as the abscissa line (1)). Thus curves 3, 4 indicate here the potential difference melt/graphite and diamond/graphite. With curves 6 and 7 are introduced the thermodynamic potential differences of two vitreous carbon forms—one we synthesized from furfuril resins, and a commercial product, respectively. Here as in a) both $G(T)$ and $\Delta G(T)$ refer to bulk materials. Note that considerable values of $\Delta G_{v/gr}$ and $\Delta G_{v/d}$ when compared with the difference $\Delta G_{d/gr}(T) = G_d(T) - G_{gr}(T)$, given with curve 2. (c) The same Gibbs potential differences as in (b). However here 6′ and 7′ refer to vitreous carbon glasses brought to nano-size dimensions. The potential difference $\Delta G(T)$ for nano-sized diamond vs. bulk graphite is introduced with curve 8. Note the change of the interception points: with Simon's $\Delta G(T)$-(curve 2 for bulk material) and when nano-size materials are used (curve 6′, 7′ and 8).

We propose here a isothermal method of metastable diamond growth where vitreous carbons and other carbon materials, representing thermodynamically non-equilibrium states of frozen-in disorder (such as soot, medical carbons, nano-dispersed diamond powders etc.) are used as a constant driving source of crystallization, additionally assisted by the high dispersity of the material. In experimental realization of this thermodynamic possibility both transport in hydrogen plasma in isothermal CVD experiments as well as several chemical gas transport reactions, taking place in the closed volume of quartz ampoules at constant temperature were used.

2. Theoretical background

The method reported here is based on the thermodynamic analysis of the non-equilibrium forms of carbon [15]: especially of various vitreous carbons and of crypto-crystalline carbon materials (such as soot), diamond dust in micro and nano-sized dispersion etc. The results are summarized on Fig. 1, giving the temperature course of thermodynamic potential of graphite, diamond, liquid carbon and different forms and dispersities of vitreous carbon materials. They are constructed taking into account the well known thermodynamic properties of crystalline graphite and diamond [16, 17] (curves 1 and 2) and in estimating the thermodynamic properties of the still hypothetical liquid carbon melt (curve 3) from general theoretical considerations (described in details in [18, 19]) and from the analogy with other Fourth Group elements (Si, Ge, Sn, Pb). Curve 4 represents the course of the thermodynamic potential of hypothetical carbon glass, if it could be obtained as a frozen-in, non-equilibrium system from the undercooled carbon melt.). Such carbon glasses could be formed, e.g., at extreme splat cooling rates from the melt (if such an experiment should be possible at kbar pressures), or as reported here: as the solid $C/H_2/H^*$ plasma—born amorphous carbon droplets we have synthesized in CVD-experiments. On the insert (curve 5) the thermodynamic potential of carbon vapours is given. On Fig. 1b the respective differences $\Delta G(T)$ (according to crystalline graphite) are constructed. With curve 2 the temperature dependence of the thermodynamic potential difference diamond/graphite is indicated [20, 21]. Curves 6 and 7 represent the $\Delta G(T)$-course for two samples of amorphous materials, called vitreous carbons, experimentally

determined from our own or from existing caloric and solubility measurements [15, 22, 23].

It is obvious from Fig. 1b that the commercially known vitreous carbon materials although having a frozen-in structure are far from the expected properties of the hypothetical carbon glass, given with curve 4. This is explained by the circumstance that these vitreous-like carbon materials are not obtained directly from the carbon melt, but are the result of processes of high temperature pyrolysis of organic resins. Their structure is known to be in fact a combination of distorted sp^2 and sp^3 bonded carbon regions intermingled with cripto-crystalline graphite regions [24]. The $\Delta G(T)$-course of these and similar vitreous carbons, as seen on Fig. 1b (curves 6 and 7), intercepts the $\Delta G(T)$-curve of the diamond/graphite equilibrium (curve 2) at temperatures between 600 K and 800 K. At temperatures below this point the *vitreous carbon → diamond* transformation should be possible; at higher temperatures diamond is more stable than the respective carbon glass. This is in essence the main idea of our method.

It turned out in our experiments that temperatures below 800 K are too low to guarantee sufficient reaction rates with the gaseous transport reactions employed. So in order to use vitreous carbon materials as a source of supersaturation in metastable diamond growth experiments the thermodynamic differences indicated on Fig. 1b have to be increased by an additional method: for instance by dispersing the precursor materials to nano-size dimensions (by milling and similar mechano-chemical procedures).

Applying the well-known Thomson-Gibbs formula $\Delta G^* = (2\sigma V_m/R)$ giving the increased thermodynamic potential ΔG^* of a solid cluster of radius, R, having interface energy, σ, in respect to the surrounding phase, vertical shift of the $\Delta G(T)$-curves to higher potential values is to be expected. Introducing $R = 10$ nm and applying reasonable values for σ (20 J/m^2 for diamond, 15 J/m^2 for graphite) and for the molar volume V_m (3.4 cm^3/mol for diamond, 5.2 cm^3/mol for graphite) of the corresponding carbon phases we constructed the $\Delta G(T)$ lines, given on Fig. 1c (6′ and 7′). Thus the interception points of the $\Delta G(T)$-curves for vitreous carbons with the $\Delta G(T)$-curve for diamond appear at considerably higher temperatures. Curve 8 on Fig. 1c gives the thermodynamic potential of nano-dispersed diamond dust.

In the experimental realization of the above outlined thermodynamic possibility additional kinetic factors have to be taken into account. The first factor is connected with introduction of seed crystals in the system. According to the kinetic treatment of Ostwald's Rule of Stages [7, 8], initiated by Stranski and Totomanov [9], the respective nucleation rates determine the predominant formation of one of two possible modifications (a stable and a metastable one). Thus in the framework of the general nucleation theory as it is outlined in [19] the kinetic condition

$$(\Phi_{gr}/\Phi_d)(\sigma_{gr}/\sigma_d)^3\left(V_m^{gr}/V_m^d\right) > (\Delta G_{v/gr}/\Delta G_{v/d}) > 1$$

has to be fulfilled for the predominant formation of metastable phase (here—of diamond). Here σ_{gr} and σ_d indicate the corresponding surface energies in respect to the gaseous phase and Φ is the nucleation activity of seed crystals introduced in the system [7, 8] (in general: $0 \leq \Phi \leq 1$). As far as $(\Delta G_{v/gr}/\Delta G_{v/d}) \approx 1$ (as it is seen from Fig. 1a), the fulfilment or not fulfilment of above condition becomes dominantly dependent only on the value of Φ: i.e., whether diamond (than $\Phi_d = 0$) or graphite (than $\Phi_{gr} = 0$) was introduced as the seed crystal in the system.

The second, significant kinetic factor to be accounted for is determined by the mechanism of incorporation

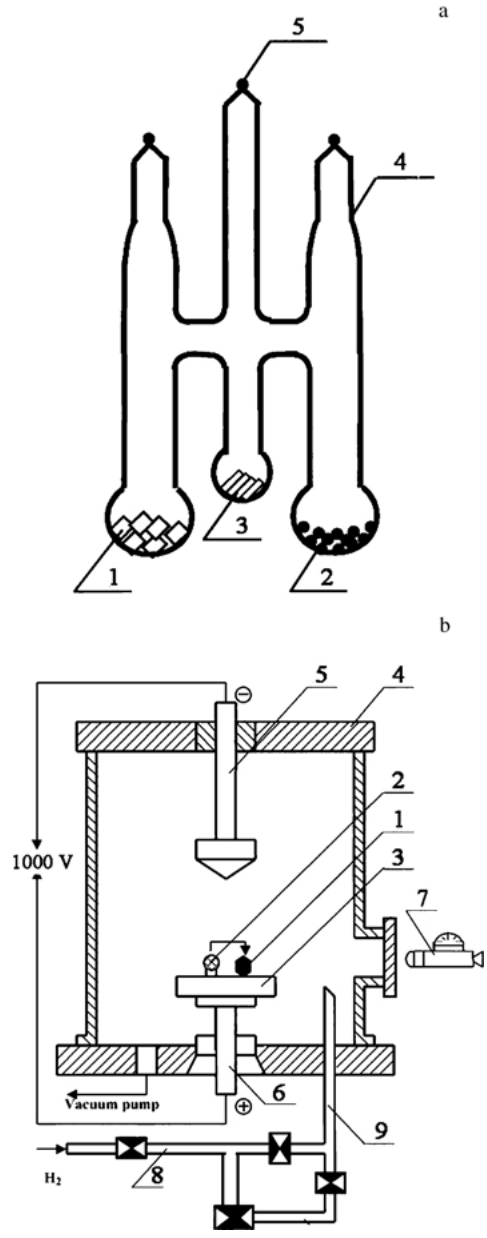

Figure 2 The two experimental arrangements employed in the experimental realization of the isothermal transformation *vitreous carbon → diamond*, *glassy carbon → diamond:* via gas transport reaction (a) or plasma assisted gas transport reaction (b). (a) Quartz ampoule for the gaseous transport realization of the *vitreous carbon → diamond* transition: (1) Seed diamonds; (2) micro-sized vitreous carbon; (3) catalysator; (4) transport gas filled ampoule; (5) sealed ampoule inlet. (b) Vacuum chamber for hydrogen—plasma assisted transformation *carbon glass → diamond*: (1) seed diamond; (2) hydrogen CVD plasma-born glassy carbon sphere; (3) Mo—substrate at 1,400 K; (4) vacuum chamber filled with hydrogen; (5) cathode; (6) anode; (7) optical hot filament pyrometer; (8, 9) inlet system for hydrogen (and when necessary of Methane or other carboneous gases).

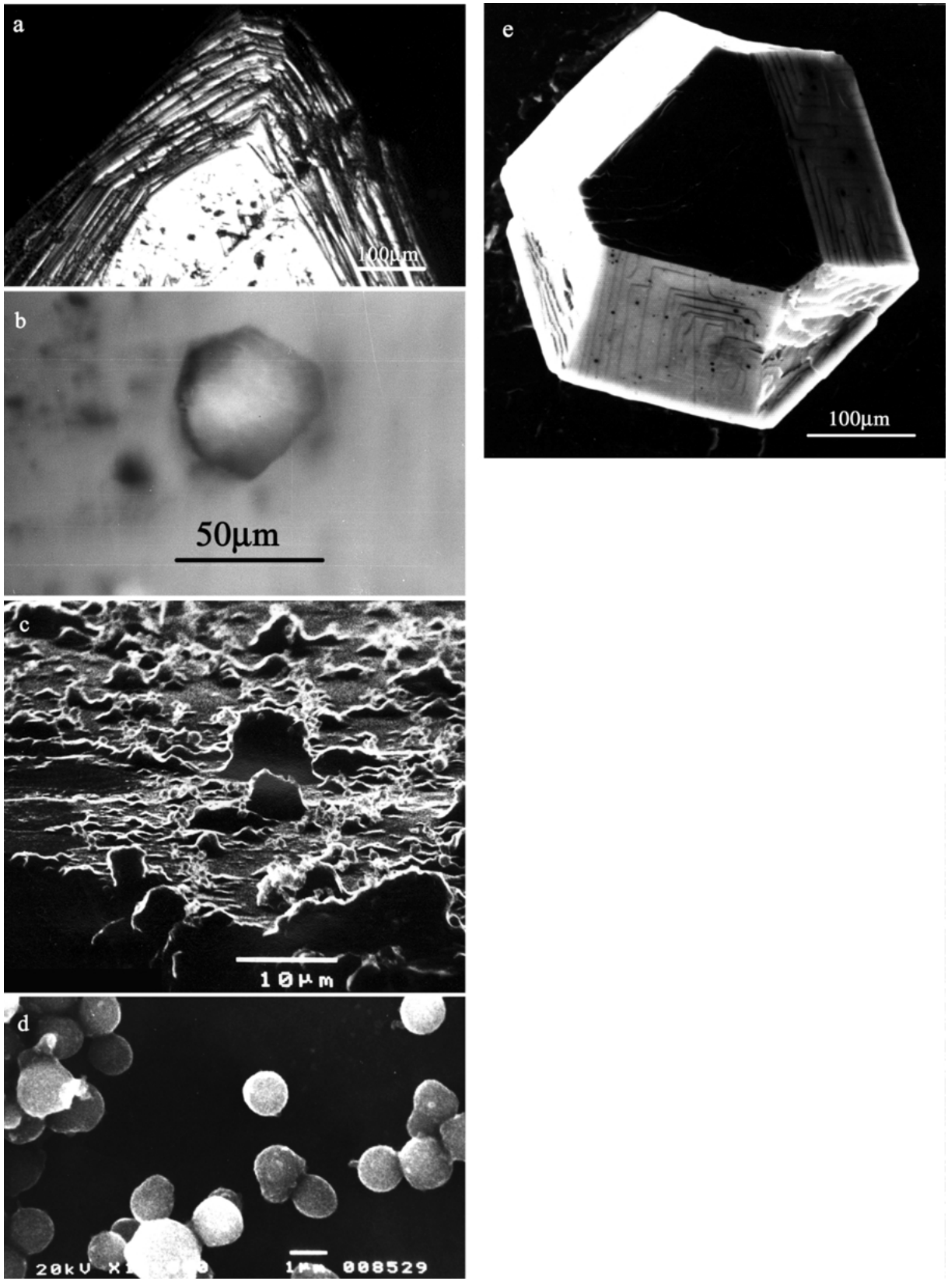

Figure 3 Growth of diamond crystals as revealed by microscopic observation (a, b, c, d—in quartz ampoule growth; e—in plasma vacuum chambre). (a) Continuous growth of diamond seed crystal (50 h at 1,259 K) with iodine vapor—transport, from micro-crystallized diamond precursor material. Note also several growth pyramids. (b) Formation of a diamond microcrystal (75 h at 1250 K) on a seed diamond surface with sulfur transport, from micro-dispersed vitreous carbon precursor. (c) Graphite formation, intermixed with an amorphous condensate on seed diamond sample, cycled several times between 800 and 1250 K (sulfur-transport gas, from micro-sized vitreous carbon). (d) Formation of vitreous carbon microspheres on diamond seed crystal at lower temperatures (50 h at 1,050 K) with J_2-transport from micro-sized vitreous carbon precursor. (e) Diamond crystal growth in hydrogen-plasma experiments in vacuum chamber (8 h at 1,400 K); demonstration of growth from a glassy carbon sphere. a, b—optical microscopic pictures; c, d, e—SEM observation.

of ambient phase molecules into the growing diamond face, depending mainly on chemical transport reactions employed. Because of the enormous strength of the C–C bonding the direct incorporation of vapour phase C atoms at the desired relatively low temperatures (1000–1400 K) into the diamond lattice is very improbable. Detailed investigations of the system $C/H_2/H^*$ show that most probably at plasma conditions the hydrogen atoms $\langle H^* \rangle$ are absorbed on diamond surface, occupying active growth sites C^*. Then incorporation of new carbon atoms is realized via the reaction [3, 6, 9] $C\langle H^* \rangle + H^* \rightarrow C^* + H_2 \uparrow$ giving "dangling bond" diamond sites and molecular hydrogen. At temperature about 1200 K this process is much more easier than the direct incorporation of C atoms into the diamond face (see also [25])—a process only possible with very highly activated C^* atoms in the vapour phase [26]. The incorporation of carbon atoms at relatively low temperatures can be additionally enhanced by the presence of halogen atoms [27]. Via the reaction $H_2 + Cl^* \rightarrow H^* + HCl$ they can catalyse the formation of atomic hydrogen at lower temperatures.

3. Experimental procedure

In a series of experiments we succeed to realize the expected *vitreous carbon → diamond* transformation, using several gas transport reactions. The first experimental realisation we obtained in sealed quartz ampoules with the construction, given on Fig. 2a. The seed crystals (natural or synthetic diamonds of 0.01 mm to 0.1 mm, sometimes in the form of larger polished brilliants), preliminarily weighted on a sensitive microbalance, were placed on the one hand side of the ampoule. On the other hand side of the ampoule the precursor carbon material was placed, usually in the form of fine-grained powder (size of grains between 10 and 100 nm). Besides the already mentioned vitreous carbons, as carbon precursor material also some other materials with different degrees of crystallinity, structure and dispersity were tested: different blends of soot, medical carbons and nano-dispersed diamond powders. In any of these materials owing to defect structure and nano—size dimensions an increased thermodynamic potential is frozen—in. The good results obtained with diamond powders may be of principal technical interest, as they demonstrate the possibility to exploit for diamond growth directly the ΔG^* difference, determined only by size effects via the already mentioned Thomson-Gibbs equation. With these nano-sized diamond precursor samples the kinetic problems connected with the $sp^2 \rightarrow sp^3$ transformation are to a great extent eliminated and smooth diamond growth was easily achieved.

For realisation of the transformation *precursor carbon material → diamond* in the closed volume of the quartz ampoules several gas-transport reactions were used. Besides the conventional $CH_4/H_2/H^*$ system (in which H^*-atoms formation was catalysed by a heated Pd-foil) with greater success several other transport reactions were used: $C + 2I_2 \rightarrow CI_4$, $C + 2Br_2 \rightarrow CB_{r4}$, $C + S \rightarrow CS_2$ etc. (known from previous experiments,

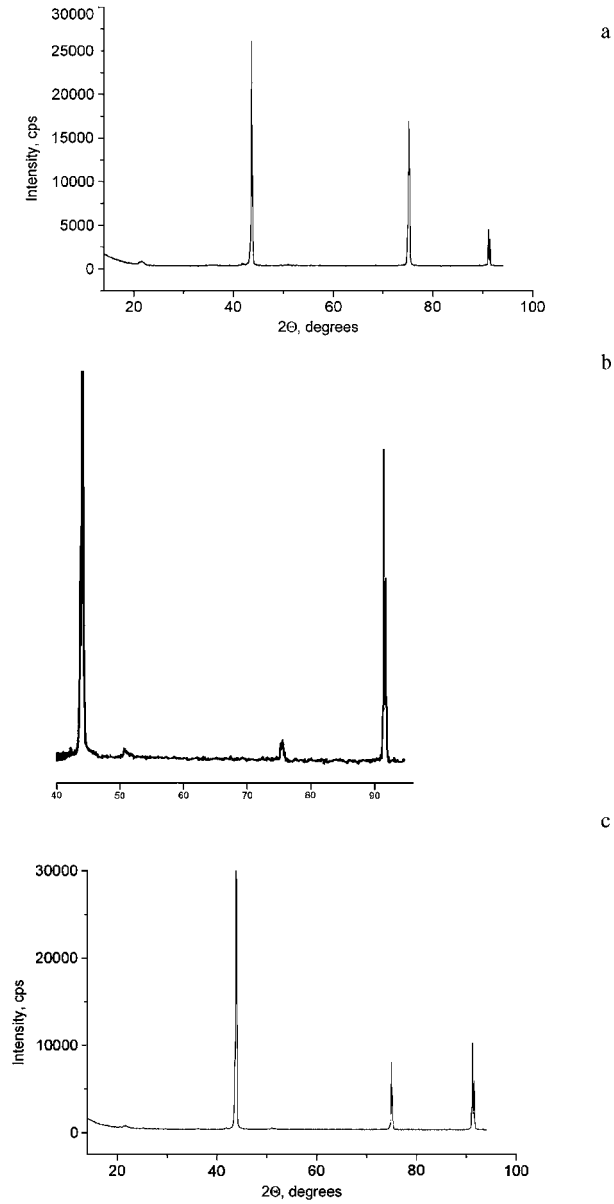

Figure 4 (a) The X-ray patterns of an assembly of small technical synthetic precursor diamonds (50 μm) used in the experiments before treatment. (b) The X-ray patterns of crystals nucleated and grown from the H-plasma apparatus. (c) The X-ray pattern of the precursor diamonds after ampoule growth.

see [3, 4]). The desired gaseous phase was formed by introducing the necessary reagents in solid form (e.g., sulphur, iodine, CBr_4, paraffin) in small quartz tubes, which cracked in the initially evacuated quartz ampoules upon heating.

Another possibility in demonstrating the *vitreous carbon → diamond* transformation was by using a conventional vacuum plasma apparatus with the construction, given on Fig. 2b. At the first stage of this experiment we obtained via the CVD condensation process glassy carbon droplets at relatively low substrate temperature (1073 K), using a mixture of hydrocarbons as a precursor carbon material. At the second stage on the Mo-anode of the same CVD vacuum apparatus (initially evacuated and than filled with H_2-gas) one of thus plasma-synthesised glassy carbon samples and a diamond single crystal were mounted, both having dimensions of approximately 1 mm (Fig. 2b). In the closed

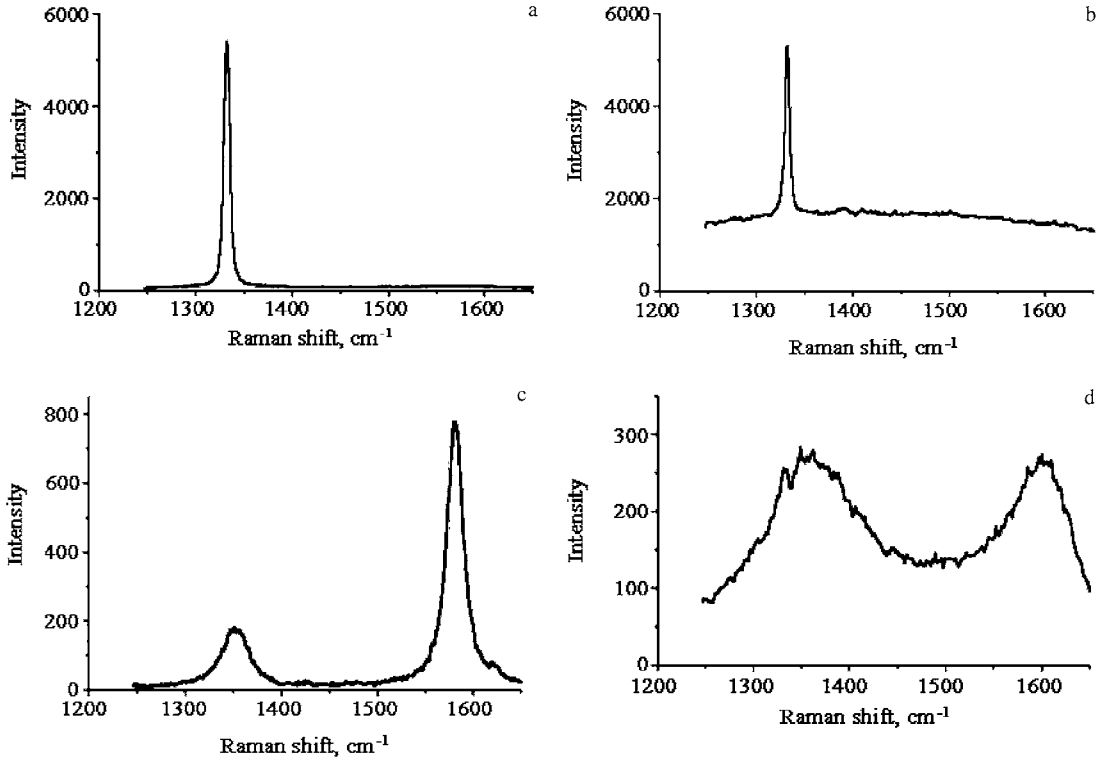

Figure 5 Typical Raman spectra of various carbon condensates investigated: (a) Diamond over-growth on synthetic diamond seed crystal; (b) diamond over growth on natural diamond seed crystal. Note here the additional luminescent Raman background characteristic of natural diamonds. (c) graphite condensation (right hand peak) and amorphous material (left hand peak); (d) vitreous carbon condensate (amorphous microspheres, cf. Fig. 3d).

volume of the vacuum chamber a hydrogen plasma was triggered (at 1000 V) and at temperature of the substrate 1400 K, in this surrounding, the carbon glass sample was isothermally fully transformed into the diamond single crystal.

4. Results and discussion

The isothermal ampoule growth experiments with vitreous carbons and the other mentioned precursor carbon materials were performed in the range of 1000 K to 1400 K at approximately 1bar and with a duration from 12 to 150 h. As a result diamond growth rates of ~ 0.5 μm/h were achieved, leading (at optimal supersaturations $\gamma = (\Delta G_{\text{v.carbon/d}}/RT)$ e.g., at $\gamma \sim 0.01$) to the smooth growth of the introduced diamond seed crystals (Fig. 3a). At higher supersaturations ($\gamma \sim 0.1$–0.2) beside continuous growth also the formation of typical diamond growth pyramids or diamond single crystallites was observed (Fig. 3a, b), thus indicating secondary nucleation. This is, as far as we known, the first proof of the *vitreous carbon* $\rightarrow$ *diamond* synthesis at metastable conditions and constant temperatures. At further increased supersaturations the dominant formation of graphite structures on the diamond seed crystals followed (Fig. 3c). At lower temperatures usually carbon glass-like condensates were also observed (the micro-spheres on Fig. 3d).

Highest growth rates and the formation of smooth epitaxial diamond or diamond-like films in the ampoule growth arrangement were obtained with the above mentioned iodine and sulphuric gaseous transport reactions, followed in efficiency by the $CH_4/H_2/H^*$ system. A thermochemical analysis revealed that this sequence is determined by the percentage of atomic reagent (H^*, S^*, I^*), present in the system (depending on the strength of the respective H–H, S–S, I–I or C–H, C–S, C–I etc. bonding, decreasing from H to I). The formation of atomic hydrogen in the $CH_4/H_2/H^*$ systems is connected with considerable difficulties because of the strength of the H–H bonding (requiring either hydrogen plasma [10, 11, 27] or an extremely hot (up to 3,500 K) filament source of activation [3, 6, 10, 27]. This is why also other gaseous reactions were tested. In some respect systems $CI_4/I_2/I^*$ and $CS_2/S_2/S^*$ repeat at lower temperature the thermochemistry of the $CH_4/H_2/H^*$ system at 3000 K, because of the decreased chemical bonding there.

At the above described CVD-arrangement experiments considerably higher growth rates (approximately 100 μm/h) were observed (Fig. 3e). These experiments also indicate that in fact via vacuum-plasma condensation glassy carbon droplets were produced, corresponding in their thermodynamic properties to the temperature course, depicted with curve 4 on Fig. 1.

In order to proof diamond growth as a result of our experiments some complimentary methods and techniques were used. The growth of the individual seed crystals was followed by exact weight measurements (performed with an accuracy of $\pm 2.10^{-6}$g), by X-ray and electron RHE-diffraction (confirming the crystalline nature of the condensate) and by UV-induced luminescent microscopy investigations.

Fig. 4a gives the X-ray patterns of an assembly of small technical synthetic precursor diamonds (50 μm mean size) used in the experiments before growth treatment. The next picture (Fig. 4b) gives the X-ray patterns of crystals like those given on Fig. 3e), nucleated and grown from the H-plasma apparatus (Fig. 2b) clearly demonstrating their diamond structure. Lastly, (Fig. 4c) shows the X-ray pattern of the precursor diamonds after the described ampoule growth: again the diamond structure is demonstrated. However, as expected it also turned out that formation of separated tiny graphite micro-crystals at the precursor diamond surface at conditions where this form of carbon condensates prevailed (see Fig. 3c), was not registered by X-ray analysis. This is why as our most efficient method of result analysis micro-Raman spectrography was used.

With the last method diamond overgrowth could be detected when natural diamond seed crystals were used: synthetic overgrowth layers from our experiments showed no luminescence. Decisive in differentiating in between different structures of the condensate in our experiments was, however, Raman spectroscopy [28], used in a microscopic laser beam arrangement. Typical Raman spectra, we obtained, are given on Fig. 5.

EDX and WDX microanalyses were performed to verify the chemical composition of condensates. For the case of $CI_4/I_2/I^*$ and $CH_4/H_2/H_4^*$ systems only traces of iodine (below 0.01%) were thus found. However, it turned out that with sulphur as a carrier gas considerable amounts (up to 1–2%) sulphur can be introduced into the growing epitaxial diamond films. When micro-dispersed diamond precursor materials, milled in a W-carbide milling apparatus were used, also W-contamination were introduced with the sulphur transport reaction.

5. Conclusions

Specific advantage of the method for diamond growth, reported here is that in the ampoule growth method, the supersaturation applied is determined only by the actual temperature of experimentation, predestining (at given structure and dispersity of precursor carbon material) the interception point and the spread of the respective $\Delta G(T)$-vitreous carbon/graphite, $\Delta G(T)$-diamond/graphite curves (see Fig. 1). The technical advantages of such procedure of isothermal growth at relatively low temperatures and normal pressures, at which the process is realized at an apparative arrangement (see Fig. 2a), are obvious. Low growth rates of both diamond single crystals (even as precut brilliants) or of thin diamond films give advantages in obtaining smooth, defect free faces. Of particular significance is also that these experiments give a direct conformation of the thermodynamic non-equilibrium state and relative stability of vitreous and crypto-crystalline forms of carbon.

Our thermodynamic diagrams (Fig. 1) and the experimental results reported here on the different forms of carbon condensation under differing conditions may be also of interest in explaining processes of carbon condensation as graphite, as glass and as diamond in natural processes taking place e.g., in interstellar space [29, 30] and of the formation of diamond micro-crystals, found in meteorites [31] or geological conditions.

Acknowledgements

We thank Dr. D. Radev and Dr. V. Bluskov (Sofia) who are mostly responsible for the mechano-chemical treatment of carbon precursor samples. We thank also to Dr. B. Bogdanov (Bourgas) for the olivine melt series experiments and I. Borsukov for the hundreds of quartz ampoules, he prepared for the investigation. Our work was supported by an International Alexander von Humboldt Research Prize, awarded to one of us (I.S.G.).

References

1. F. P. BUNDY, *J. Chem. Phys*. **38** (1963) 631.
2. F. P. BUNDY, H. M. STRONG and R. H. WENTORF Jr., in "Chemistry and Physics of Carbon," edited by P. L. Walker Jr. and P. A. Thrower, Vol. 10 (Marcel Dekker Inc., New York, 1973) p. 213.
3. J. C. ANGUS, A. ARGOTIA, R. GAT *et al*., in "Thin Film Diamond," edited by A. Lettington and J. W. Steeds (The Roy. Soc., Chapman & Hall, London, 1994) p. 1.
4. B. V. DERJAGUIN and D. V. FEDOSEEV, *Carbon* **11** (1973) 299.
5. R. C. DE VRIES, *Rev. Mater. Sci*. A **17** (1987) 161.
6. R. SAUER, *Cryst. Res. Technol*. **34** (1999) 227.
7. I. GUTZOW and J. SCHMELZER, "The Vitreous State: Thermodynamics, Structure, Rheology and Crystallization" (Springer, Berlin, New York, 1995) p. 375.
8. I. GUTZOW and I. AVRAMOV, *J. Non-Cryst. Solids* **16** (1974) 128.
9. I. N. STRANSKI and D. TOTOMANOW, *Z. Phys. Chem*. A **163** (1933) 399.
10. P. R. BACHMANN, in "Thin Film Diamond," edited by A. Lettington and J. W. Steeds (The Roy. Soc., Chapman & Hall, London, 1994) p. 30.
11. Y. Z. WAN, D. W. ZHANG, Z.-J. LIN *et al*., *J. Appl. Phys*. A **67** (1998) 225.
12. L. KOSTADINOV, D. DOBREV, K. OKANO *et al*., *Diam. and Rel. Mater*. **1** (1992) 157.
13. E. GRANTSCHAROVA and I. GUTZOW, *J. Non-Cryst. Solids* **81** (1986) 99.
14. I. GUTZOW, D. ILIEVA, F. BABALIEVSKI and V. YAMAKOV, *J. Chem. Phys*. **112** (2000) 10941.
15. V. GUENCHEVA, E. GRANTSCHAROVA and I. GUTZOW, *Cryst. Res. Techn*. **36** (2001) 1411.
16. O. KNACKE, O. KUBASCHEVSKI and K. HASSELMANN (eds.), "Thermochemical Properties of Inorganic Substances" (Springer, Berlin, New York, 1991) p. 264.
17. F. P. BUNDY, *J. Chem. Phys*. **38** (1963) 618.
18. I. GUTZOW and A. DOBREVA, *J. Non-Cryst. Solids* **129** (1991) 266.
19. I. GUTZOW and J. SCHMELZER, "The Vitreous State: Thermodynamics, Structure, Rheology and Crystallization" (Springer, Berlin, New York, 1995) p. 67.
20. R. BERMAN and F. SIMON, *Zs. Elektrochem*. **55** (1956) 344.
21. F. P. BUNDY *et al*., *J. Chem. Phys*. **35** (1961) 383.
22. L. F. VERESHCHAGIN, E. N. YAKOVLEV, L. M. BUCHNEV and B. K. DYMOV, *High Temperature Thermophysics* **15** (1977) 316 (in Russian).
23. W. WEISWEIHLER and V. MAHADEVAN, *High Temperatures-High Pressures* **3** (1971) 111.
24. C. D. WIGNALL and C. J. PINGS, *Carbon* **12** (1974) 51.
25. W. PIEKARCZYK, R. MESSIER and R. ROY, *J. Cryst. Growth* **106** (1990) 279.

26. A. V. PAVLICHENKO, A. M. JONAS, J.-C. CHARLIER *et al*., *Nature* **402** (1999) 162.
27. D. E. PATTERSON *et al*., in "Applications of Diamond Films and Related Materials," edited by Y. Tzeng, M. Yoshikawa, M. Murakawa and A. Feldman (Elsevier Science Publishers B. V., 1991) p. 569.
28. P. V. HUONG, in "Diamond and Diamond Like Carbon Coatings," 1990, edited by A. Matthews and P. K. Bademann (Elsevier Sequoia, Lausane, New York, 1991) p. D12.
29. W. C. SASLAW and J. E. GAUSTAD, *Nature* **221** (1969) 160.
30. H. MUTSCHKE, J. DORSCHNER and TH. HENNING, *Astrophys. Journ*. **454** (1995) L 157.
31. U. OTT, *Nature* **364** (1993) 25.
32. T. HARAHARA and N. FUJIMORI, *Mat. Res. Innov*. **1** (1997) 38.

Received 11 December 2002
and accepted 10 June 2003